

Direct observation of anisotropic Cooper pairing in kagome superconductor CsV₃Sb₅

Akifumi Mine¹, Yigui Zhong^{1,*}, Jinjin Liu^{2,3}, Takeshi Suzuki¹, Sahand Najafzadeh¹, Takumi Uchiyama¹, Jia-Xin Yin⁴, Xianxin Wu⁵, Xun Shi^{2,3}, Zhiwei Wang^{2,3,6}, Yugui Yao^{2,3,6}, Kozo Okazaki^{1,7,8,*}

¹*Institute for Solid State Physics, The University of Tokyo, Kashiwa, Japan*

²*Centre for Quantum Physics, Key Laboratory of Advanced Optoelectronic Quantum Architecture and Measurement (MOE), School of Physics, Beijing Institute of Technology, Beijing, China*

³*Beijing Key Lab of Nanophotonics and Ultrafine Optoelectronic Systems, Beijing Institute of Technology, Beijing, China*

⁴*Department of Physics, Southern University of Science and Technology, Shenzhen, China*

⁵*CAS Key laboratory of Theoretical Physics, Institute of Theoretical Physics, Chinese Academy of Sciences, Beijing, China*

⁶*Material Science Center, Yangtze Delta Region Academy of Beijing Institute of Technology, Jiaxing, China*

⁷*Trans-scale Quantum Science Institute, The University of Tokyo, Tokyo, Japan*

⁸*Material Innovation Research Center, The University of Tokyo, Kashiwa, Japan*

*Corresponding to: yigui-zhong@issp.u-tokyo.ac.jp; okazaki@issp.u-tokyo.ac.jp

Abstract

In the recently discovered kagome superconductor AV₃Sb₅ (A = K, Rb, and Cs), the superconductivity is intertwined with an unconventional charge density wave order. Its pairing symmetry remains elusive owing to the lack of direct measurement of the superconducting gap in the momentum space. In this letter, utilizing laser-based ultra-high-resolution and low-temperature angle-resolved photoemission spectroscopy, we observe anisotropic Cooper pairing in kagome superconductor CsV₃Sb₅. We detect a highly anisotropic superconducting gap structure with an anisotropy over 80% and the gap maximum along the V-V bond direction on a Fermi surface originated from the 3d-orbital electrons of the V kagome lattice. It is in stark contrast to the isotropic superconducting gap structure on the other Fermi surface that is occupied by Sb 5p-orbital electrons. Our observation of the anisotropic Cooper pairing in pristine CsV₃Sb₅ is fundamental for understanding intertwined orders in the ground state of kagome superconductors.

Kagome lattice is a combination of corner-shared triangles and hexagons. Such a unique structure causes geometrical frustration in the spin degree of freedom and the destructive quantum interference in the electronic wavefunctions [1-3]. The latter generates the localized density of states inside the hexagons and introduces a topological flat band. In addition, because of the similar group symmetry with graphene, there are a Dirac cone and van Hove singularities (VHS) in the electronic band structure. Therefore, kagome lattice materials provide an ideal platform for studying the interplay between topology, correlations, and the emergent novel electronic orders [4-6]. While the kagome lattice materials have existed for a long time, AV_3Sb_5 ($A = K, Rb$, and Cs) with a kagome lattice was recently discovered to be a superconductor, in which many interesting phenomena [7-9], such as giant anomalous Hall effect [10,11], unconventional charge density wave (CDW) [12-15], electronic nematicity [16-18], and pair density wave [19,20], have been observed. Owing to these exotic phenomena, AV_3Sb_5 family superconductor attracts considerable attentions and is being intensively studied.

As a new superconductor with novel physical properties, one of the most important issues is the superconducting (SC) gap symmetry because it is fundamental in clarifying the microscopic pairing mechanism and interplays between multiple electronic orders. Our previous ARPES studies on niobium-doped $Cs(V_{0.93}Nb_{0.07})_3Sb_5$ and tantalum-doped $Cs(V_{0.86}Ta_{0.14})_3Sb_5$ suggest an isotropic and nodeless SC gap structure in both cases [21]. Such a SC gap structure gets in line with the observations of the Hebel-Slichter coherent peak in the spin-lattice relaxation rate revealed by the NMR studies of CsV_3Sb_5 [22] and the exponentially temperature-dependent magnetic penetration depth [23,24]. However, certain V-shaped gaps, as well as residual Fermi-level states measured by scanning tunnelling spectroscopy [19,25,26] in CsV_3Sb_5 seem to support a scenario of the anisotropic SC gap structure. Moreover, it has been reported that the anisotropy in the SC gap of CsV_3Sb_5 can be suppressed by chemical substitution or impurity injection [27,28]. Therefore, to pin down the gap symmetry, the direct measurement of the SC gap structure in non-doped CsV_3Sb_5 is highly desired.

In this study, we have used ultra-high resolution and low-temperature laser-based angle-resolved photoemission spectroscopy (ARPES) to directly measure the SC gap in the momentum space of kagome superconductor CsV_3Sb_5 [29]. We choose high-quality single crystals which has a relatively higher SC transition temperature $T_c \simeq 3.2$ K [29] to ensure the accuracy of the SC gap measurements. Figure 1(a) shows the crystal structure of CsV_3Sb_5 , which belongs to the space group P6/mmm. The vanadium atoms form a kagome lattice. As the phase diagram shown in Fig. 1(b), in addition to the SC transition, CsV_3Sb_5 has a CDW transition around $T_{CDW} \simeq 94$ K. The SC phase has two domes with applying pressure and chemical doping [30-32], implying an unconventional interplay between SC and CDW orders. The inset of Fig. 1(b) shows the schematic Fermi surface (FS) of CsV_3Sb_5 , comprising a circular pocket and hexagonal pocket at the center of the Brillouin Zone (BZ), and a triangular pocket

at the BZ corner. By performing careful ARPES measurements along these three FS sheets, we observe an isotropic SC gap structure on the circular and triangular FS sheets. Strikingly, a strongly anisotropic SC gap is observed with the gap maximum along V-V bond direction on the hexagonal FS originated from the $3d$ -orbital electrons of V kagome lattice. The direct observation of the anisotropic Cooper pairing lays a foundation to comprehensively understand the pairing symmetry and mechanism of kagome superconductors.

We first map out the FS, which is important to study the SC gap structure for a multiband system. As shown in Fig. 2 (a), the ARPES intensity integration near the Fermi level (E_F) fits well with the calculated FS contours [33,34] as drawn in the inset of Fig.1(b). Following the previous study [21,35], the FS sheets in this study are marked as α , β , and δ for the central circular, hexagonal pockets, and outer triangular pockets, respectively. Figure 2(b) shows the E - k map of the purple and brown cuts in Fig. 2(a) taken by s - and p -polarized light, respectively. The bands of β FS have stronger intensity with s -polarization, while the bands of δ FS have stronger intensity with p -polarization. This clearly shows the difference in orbital components for these two FS sheets and is helpful to distinguish the bands corresponding to β and δ FS sheets.

Next, we study the SC gap in the momentum space. In Fig. 2(c)-(e), we show the symmetrized energy distribution curves (EDCs) at the Fermi momentum (k_F) positions along with α , β , and δ FS sheets. These EDCs are taken at $T = 2$ K, below T_c of approximately 3.2 K. For clarity, the k_F positions are marked as the FS angle φ defined in Fig. 2(a). While the detectable momentum of the 5.8-eV laser is restricted, the measured area spans over a 60-degree range of the FS angle, surpassing the minimum requirement for the six-fold symmetry. Clearly, the SC gap on α and δ FS is nearly isotropic as proved by the similar shallows near E_F in the symmetrized EDCs shown in Fig. 2(c) and Fig. 2(e), respectively. Remarkably, as the symmetrized EDCs of β FS shown in Fig. 2(d), the SC gap is strongly dependent with the FS angle. The maximum of the SC gap is observed at k_F positions along with Γ -M direction, while the minimum of the SC gap is observed at k_F positions along with Γ -K direction. As the temperature-dependent EDCs at k_F position of approximately 210° shown in Fig. 2(f), the SC gap is far smaller than the experimental energy resolution, suggestive of a possible node.

By fitting the EDCs to a Bardeen-Cooper-Schrieffer spectral function [29], we quantitatively extracted the SC gap magnitude. The obtained SC gap magnitude as a function of the FS angle is summarized in Fig. 3(b). The corresponding k_F positions are shown in Fig. 3(a) as open black circles. As shown in Fig. 3(b), the SC gap structure of β FS has a large anisotropy over approximately 80%, while the SC gaps on α and δ FS sheets are isotropic. The distribution of the SC gap magnitudes in the in-plane momentum space is summarized in Fig. 3(c) by symmetrizing the SC gap distribution on measured k_F positions following the six-fold symmetry.

It is of notice that by integrating the SC gaps on three FS sheets, the anisotropy is kept since the isotropic SC gaps on α and δ FS sheets do not contribute any features. Thus, our result is consistent with the overall anisotropic SC gap structure deduced from the field-angle-resolved calorimetry measurements [36], as well as the V-shaped local density of states measured by scanning tunneling spectroscopy [19,25,26]. On the other hand, the observed isotropic SC gap on α FS occupied by Sb 5p orbital electrons is consistent with the observation of Hebel-Slichter coherent peak in the spin-lattice relaxation rate from $^{121/123}\text{Sb}$ nuclear quadrupole resonance measurements [22]. Considering our previous results of the isotropic SC gap for chemically substituted CsV_3Sb_5 [21], in which the V kagome lattice is expanded by the partial substitutions of Nb or Ta with larger atomic radius, it is suggested that the anisotropy in the SC gap is sensitive to the kagome lattice geometry. This is consistent with the previous magnetic penetration depth measurements [27] reported that the SC gap becomes more and more isotropic with increasing impurities by electron irradiation.

The observed SC gap structures on these three FS sheets provide intuition that the Cooper pairing of Sb 5p electrons tends to be isotropic, while the Cooper pairing of V 3d electrons tends to be anisotropic. The isotropic SC gap is observed on α FS since it is mainly occupied by Sb 5p_z electrons [34,37,38]. While both β and δ FS sheets are mainly occupied by V 3d electrons [38,39], there is a significant difference on the SC gap structure that the δ FS has a nearly isotropic SC gap while β FS has a strong anisotropic SC gap structure. This stark difference can be understood by including the anisotropic CDW gap. According to the band calculations considering the orbital contributions [37], these two Fermi surfaces are mainly occupied by V 3d electrons but with a partial occupation from Sb 5p electrons. Furthermore, the CDW order gaps are observed for the V 3d electrons on δ FS sheet but no CDW gap is observable for β FS, evidenced by the laser-ARPES measurements [35]. Therefore, the SC gap on δ FS could be induced by pairing residual Sb 5p electrons, giving out an isotropic gap. Then, the anisotropic gap observed on β FS should be dominantly from the V 3d electronic pairing.

The observation of the anisotropic Cooper pairing in CsV_3Sb_5 kagome superconductor is in good agreement with theoretical predictions under the mechanism of paramagnon interference [40]. The unique geometrical frustration of kagome lattice prohibits the freezing of paramagnons and promotes the quantum interference among them, providing the sizable inter-site scattering. The smectic bond order is therefore realized. The bond-order fluctuations naturally mediate strong pairing glue that leads to both nodal s-wave and p-wave pairing states. Particularly, the nodal s-wave pairing state, which shows a node along ΓK direction and a maximum along V-V bond direction (ΓM), is highly consistent with our observation of SC gap structure on β FS originated from 3d electrons of V kagome lattice. Moreover, such a nodal s-wave gap can be gradually quenched by inducing nonmagnetic dilute V-site impurities, and finally lead to an isotropic gap function [40]. This, again, is highly reproduced by our previous

high-resolution ARPES observations of isotropic SC gap in 7%-Nb and 14%-Ta doped samples [21]. By summarizing these findings on pristine and chemically substituted CsV_3Sb_5 compounds, we present the experimental demonstration of such a nodal-nodeless transition in SC gap function tuned by dilute V-site impurity effects, supporting the pairing glued by bond-order fluctuations.

In summary, we have investigated the SC gap distribution in the momentum space of kagome superconductor CsV_3Sb_5 by high-resolution ARPES measurements. Remarkably, a strongly anisotropic SC gap is observed on the FS occupied by $3d$ electrons of V kagome lattice. The anisotropy is over 80% and the gap maximum occurs along V-V bond direction (ΓM direction in momentum space). Combined with our previous observations of fully isotropic SC gap in chemically substituted CsV_3Sb_5 , in which the V atoms are partially substituted by Nb or Ta atoms, the anisotropic Cooper pairing is frail to the distribution of the kagome lattice geometry. Overall, our direct observation of the strongly anisotropic Cooper pairing in kagome superconductor CsV_3Sb_5 lays a foundation to further understand the nature of kagome superconductivity.

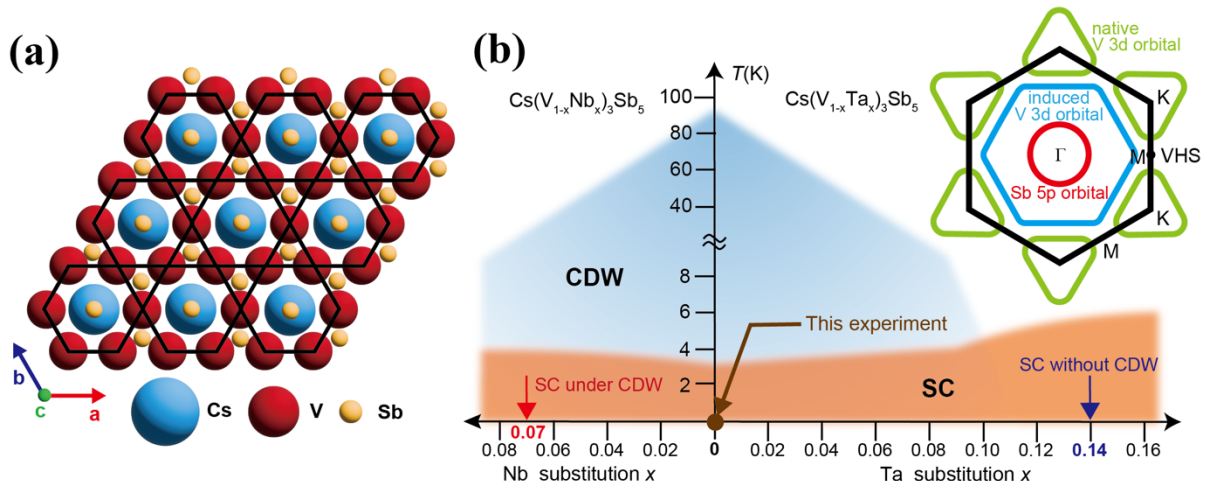


Fig. 1. **(a)** Crystal structure of CsV_3Sb_5 viewed from the perpendicular direction to the layer. **(b)** The phase diagram of CsV_3Sb_5 with Nb and Ta substitutions. SC and CDW refer to superconducting and charge density wave orders, respectively. Red and blue arrows indicate positions in the phase diagram at $\text{Cs}(\text{V}_{0.93}\text{Nb}_{0.07})_3\text{Sb}_5$ and $\text{Cs}(\text{V}_{0.86}\text{Ta}_{0.14})_3\text{Sb}_5$. Inset is a calculated Fermi surface of CsV_3Sb_5 . Each band consists of the orbits shown in the figure, and there are multiple van Hove singularities at the M point.

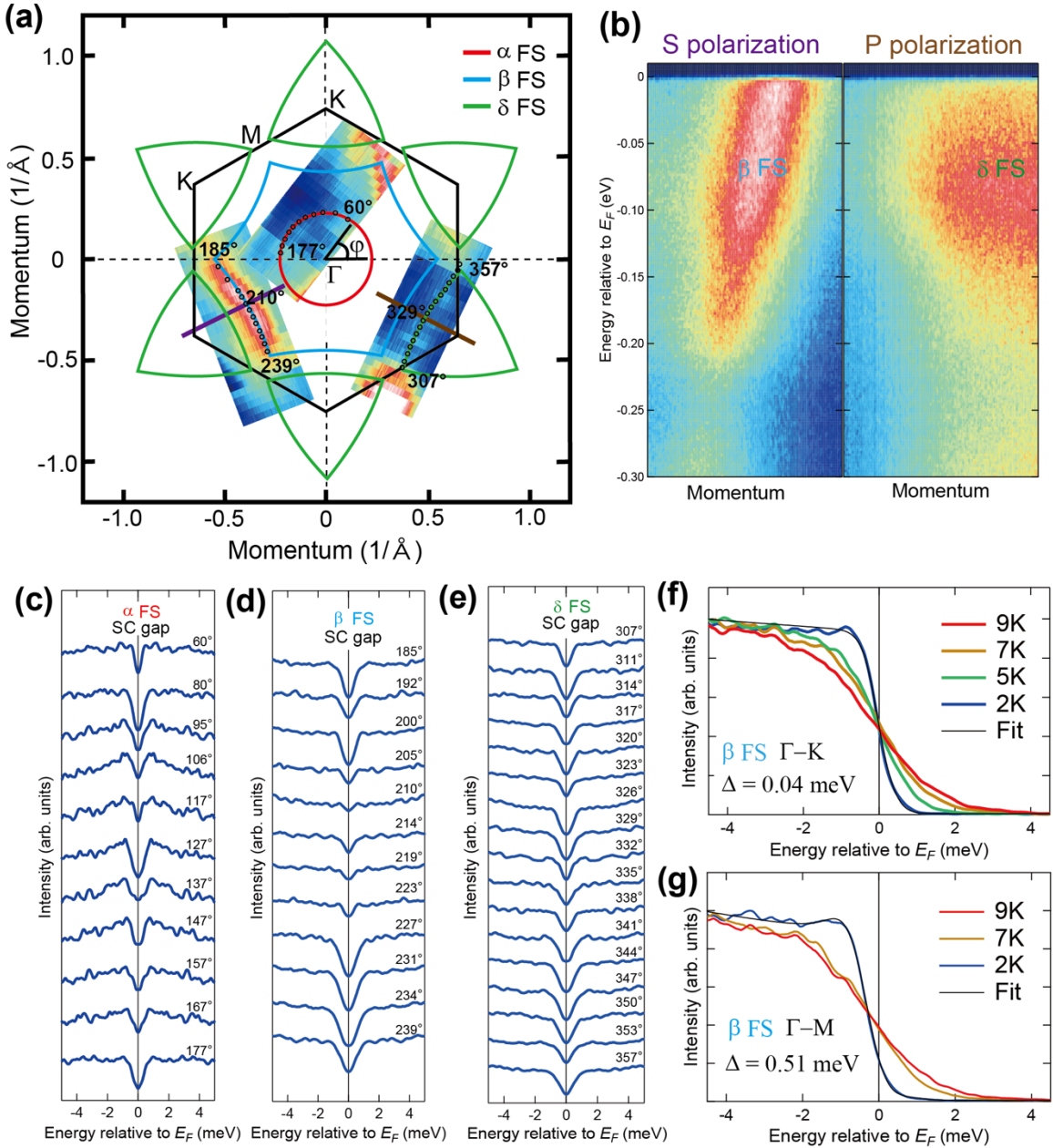


Fig. 2. **(a)** Fermi surface (FS) mapping of CsV_3Sb_5 . Color lines in the figure represents the Fermi surface contours from the band calculations. The black open circles correspond to k_F positions where the energy distribution curves (EDCs) are plotted. **(b)** Energy-momentum ($E-k$) maps along with the purple and brown cuts in **(a)** obtained with s - and p -polarization, respectively. **(c-e)** Symmetrized EDCs measured at $T = 2 \text{ K}$ in different k_F positions for α , β , and δ FS sheets, respectively. The k_F positions are marked as FS angle (φ) as defined in **(a)**. **(f)**, **(g)** Temperature dependent EDCs along with $\Gamma\text{-K}$ and $\Gamma\text{-M}$ direction on β FS, respectively. Black lines on the top of the EDCs at 2 K are the best fits to BCS spectral function.

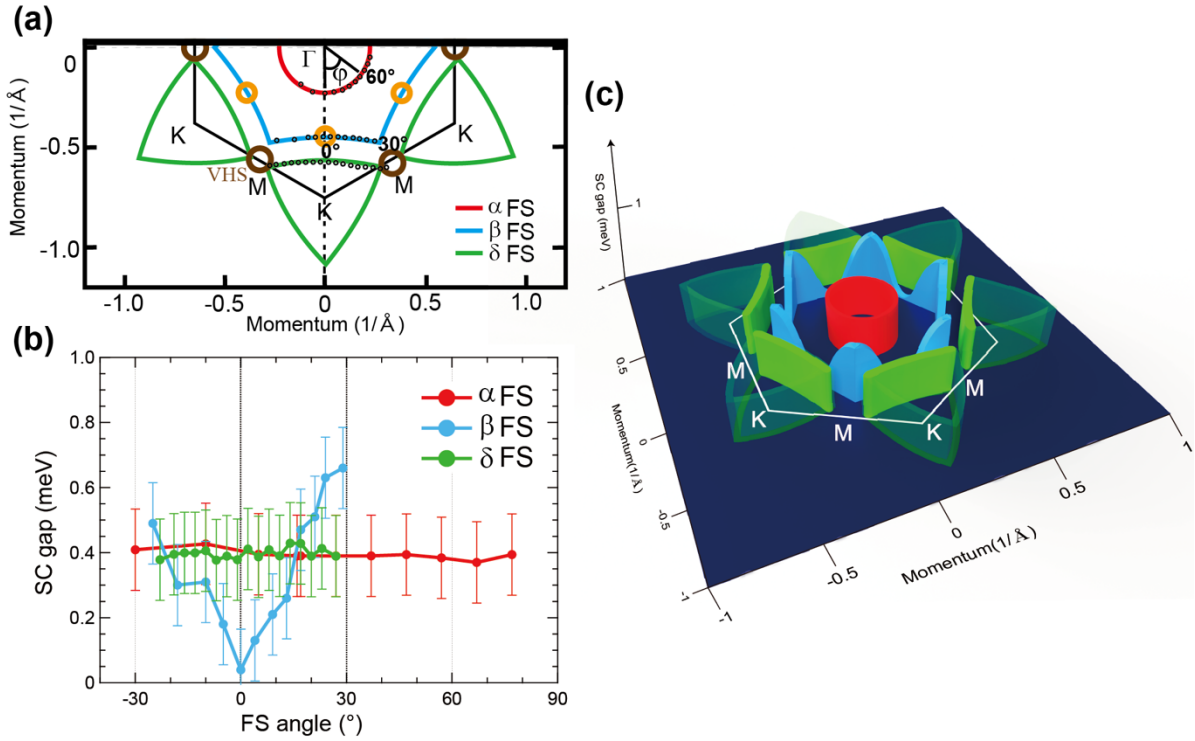


Fig. 3. (a) A summary of k_{F} positions, where the SC gap is measured. The color lines are the Fermi surface contours of CsV_3Sb_5 . **(b)** Fitted SC gap magnitudes on three FS sheets plotted as a function of FS angle (φ) as defined in **(a)**. The yellow circles in **(a)** mark the momentum positions with a minimum SC gap, while the brown circles mark the momentum location of VHS. **(c)** Schematic plot of the SC gap distribution in the in-plane momentum space of CsV_3Sb_5 .

References

- [1] I. Syôzi, Statistics of kagomé lattice, *Progress of Theoretical Physics* **6**, 306 (1951).
- [2] J.-X. Yin, B. Lian, and M. Z. Hasan, Topological kagome magnets and superconductors, *Nature* **612**, 647 (2022).
- [3] S. Yan, D. A. Huse, and S. R. White, Spin-liquid ground state of the $S=1/2$ kagome Heisenberg antiferromagnet, *Science* **332**, 1173 (2011).
- [4] S.-L. Yu and J.-X. Li, Chiral superconducting phase and chiral spin-density-wave phase in a Hubbard model on the kagome lattice, *Physical Review B* **85**, 144402 (2012).
- [5] M. L. Kiesel, C. Platt, and R. Thomale, Unconventional fermi surface instabilities in the kagome Hubbard model, *Phys. Rev. Lett.* **110**, 126405, 126405 (2013).
- [6] W.-S. Wang, Z.-Z. Li, Y.-Y. Xiang, and Q.-H. Wang, Competing electronic orders on kagome lattices at van Hove filling, *Physical Review B* **87**, 115135 (2013).
- [7] B. R. Ortiz, L. C. Gomes, J. R. Morey, M. Winiarski, M. Bordelon, J. S. Mangum, I. W. Oswald, J. A. Rodriguez-Rivera, J. R. Neilson, and S. D. Wilson, New kagome prototype materials: discovery of KV_3Sb_5 , RbV_3Sb_5 , and CsV_3Sb_5 , *Phys. Rev. Mat.* **3**, 094407 (2019).
- [8] T. Neupert, M. M. Denner, J.-X. Yin, R. Thomale, and M. Z. Hasan, Charge order and superconductivity in kagome materials, *Nature Physics* **18**, 137 (2021).
- [9] K. Jiang, T. Wu, J. X. Yin, Z. Y. Wang, M. Z. Hasan, S. D. Wilson, X. H. Chen, and J. P. Hu, Kagome superconductors AV_3Sb_5 ($A = K, Rb, Cs$), *Natl Sci Rev* **10**, nwac199 (2023).
- [10] S.-Y. Yang, Y. Wang, B. R. Ortiz, D. Liu, J. Gayles, E. Derunova, R. Gonzalez-Hernandez, L. Šmejkal, Y. Chen, and S. S. Parkin, Giant, unconventional anomalous Hall effect in the metallic frustrated magnet candidate, KV_3Sb_5 , *Science Advances* **6**, eabb6003 (2020).
- [11] F. Yu, T. Wu, Z. Wang, B. Lei, W. Zhuo, J. Ying, and X. Chen, Concurrence of anomalous Hall effect and charge density wave in a superconducting topological kagome metal, *Physical Review B* **104**, L041103 (2021).
- [12] C. Mielke, D. Das, J.-X. Yin, H. Liu, R. Gupta, Y.-X. Jiang, M. Medarde, X. Wu, H. Lei, and J. Chang, Time-reversal symmetry-breaking charge order in a kagome superconductor, *Nature* **602**, 245 (2022).
- [13] Y. Xu, Z. Ni, Y. Liu, B. R. Ortiz, Q. Deng, S. D. Wilson, B. Yan, L. Balents, and L. Wu, Three-state nematicity and magneto-optical Kerr effect in the charge density waves in kagome superconductors, *Nature Physics* **18**, 1470 (2022).
- [14] H. Li, T. Zhang, T. Yilmaz, Y. Pai, C. Marvinney, A. Said, Q. Yin, C. Gong, Z. Tu, and E. Vescovo, Observation of Unconventional Charge Density Wave without Acoustic Phonon Anomaly in Kagome Superconductors AV_3Sb_5 ($A = Rb, Cs$), *Physical Review X* **11**, 031050 (2021).
- [15] Y.-X. Jiang, J.-X. Yin, M. M. Denner, N. Shumiya, B. R. Ortiz, G. Xu, Z. Guguchia, J. He, M. S. Hossain, and X. Liu, Unconventional chiral charge order in kagome superconductor KV_3Sb_5 , *Nat. Mater.* **20**, 1353 (2021).
- [16] H. Li, H. Zhao, B. R. Ortiz, T. Park, M. Ye, L. Balents, Z. Wang, S. D. Wilson, and I.

Zeljkovic, Rotation symmetry breaking in the normal state of a kagome superconductor KV_3Sb_5 , *Nature Physics* **18**, 265 (2022).

[17] L. P. Nie, K. Sun, W. R. Ma, D. W. Song, L. X. Zheng, Z. W. Liang, P. Wu, F. H. Yu, J. Li, M. Shan *et al.*, Charge-density-wave-driven electronic nematicity in a kagome superconductor, *Nature* **604**, 59 (2022).

[18] Z. C. Jiang, H. Y. Ma, W. Xia, Z. T. Liu, Q. Xiao, Z. H. Liu, Y. C. Yang, J. Y. Ding, Z. Huang, J. Y. Liu *et al.*, Observation of Electronic Nematicity Driven by the Three-Dimensional Charge Density Wave in Kagome Lattice KV_3Sb_5 , *Nano Lett* **23**, 5625 (2023).

[19] H. Chen, H. Yang, B. Hu, Z. Zhao, J. Yuan, Y. Xing, G. Qian, Z. Huang, G. Li, Y. Ye *et al.*, Roton pair density wave in a strong-coupling kagome superconductor, *Nature* **599**, 222 (2021).

[20] H. Li, D. Oh, M. Kang, H. Zhao, B. R. Ortiz, Y. Oey, S. Fang, Z. Ren, C. Jozwiak, and A. Bostwick, Small Fermi pockets intertwined with charge stripes and pair density wave order in a kagome superconductor, *Physical Review X* **13**, 031030 (2023).

[21] Y. G. Zhong, J. J. Liu, X. X. Wu, Z. Guguchia, J. X. Yin, A. Mine, Y. K. Li, S. Najafzadeh, D. Das, C. Mielke *et al.*, Nodeless electron pairing in CsV_3Sb_5 -derived kagome superconductors, *Nature* **617**, 488 (2023).

[22] C. Mu, Q. Yin, Z. Tu, C. Gong, H. Lei, Z. Li, and J. Luo, S-wave superconductivity in kagome metal CsV_3Sb_5 revealed by $^{121/123}\text{Sb}$ NQR and ^{51}V NMR measurements, *Chinese Physics Letters* **38**, 077402 (2021).

[23] W. Duan, Z. Nie, S. Luo, F. Yu, B. R. Ortiz, L. Yin, H. Su, F. Du, A. Wang, and Y. Chen, Nodeless superconductivity in the kagome metal CsV_3Sb_5 , *Science China Physics, Mechanics & Astronomy* **64**, 107462 (2021).

[24] R. Gupta, D. Das, C. H. Mielke III, Z. Guguchia, T. Shiroka, C. Baines, M. Bartkowiak, H. Luetkens, R. Khasanov, and Q. Yin, Microscopic evidence for anisotropic multigap superconductivity in the CsV_3Sb_5 kagome superconductor, *npj Quantum Materials* **7**, 49 (2022).

[25] H.-S. Xu, Y.-J. Yan, R. Yin, W. Xia, S. Fang, Z. Chen, Y. Li, W. Yang, Y. Guo, and D.-L. Feng, Multiband superconductivity with sign-preserving order parameter in kagome superconductor CsV_3Sb_5 , *Phys. Rev. Lett.* **127**, 187004 (2021).

[26] Z. Wang, Y.-X. Jiang, J.-X. Yin, Y. Li, G.-Y. Wang, H.-L. Huang, S. Shao, J. Liu, P. Zhu, N. Shumiya *et al.*, Electronic nature of chiral charge order in the kagome superconductor CsV_3Sb_5 , *Physical Review B* **104**, 075148 (2021).

[27] M. Roppongi, K. Ishihara, Y. Tanaka, K. Ogawa, K. Okada, S. Liu, K. Mukasa, Y. Mizukami, Y. Uwatoko, R. Grasset *et al.*, Bulk evidence of anisotropic s-wave pairing with no sign change in the kagome superconductor CsV_3Sb_5 , *Nat. Commun.* **14**, 667 (2023).

[28] B. Hu, H. Chen, Y. Ye, Z. Huang, X. Han, Z. Zhao, H. Xiao, X. Lin, H. Yang, and Z. Wang, Discovery of a distinct collective mode in kagome superconductors, *arXiv preprint arXiv:2403.09395* (2024).

[29] See supplementary materials for the details on crystal growth and characterization, laser-ARPES measurements, superconducting gap fitting.

- [30] K. Chen, N. Wang, Q. Yin, Y. Gu, K. Jiang, Z. Tu, C. Gong, Y. Uwatoko, J. Sun, and H. Lei, Double superconducting dome and triple enhancement of T_c in the kagome superconductor CsV_3Sb_5 under high pressure, *Phys. Rev. Lett.* **126**, 247001 (2021).
- [31] F. Yu, D. Ma, W. Zhuo, S. Liu, X. Wen, B. Lei, J. Ying, and X. Chen, Unusual competition of superconductivity and charge-density-wave state in a compressed topological kagome metal, *Nat. Commun.* **12**, 3645 (2021).
- [32] Y. M. Oey, B. R. Ortiz, F. Kaboudvand, J. Frassineti, E. Garcia, R. Cong, S. Sanna, V. F. Mitrović, R. Seshadri, and S. D. Wilson, Fermi level tuning and double-dome superconductivity in the kagome metal $\text{CsV}_3\text{Sb}_{5-x}\text{Sn}_x$, *Phys. Rev. Mat.* **6**, L041801 (2022).
- [33] B. R. Ortiz, S. M. Teicher, Y. Hu, J. L. Zuo, P. M. Sarte, E. C. Schueller, A. M. Abeykoon, M. J. Krogstad, S. Rosenkranz, and R. Osborn, CsV_3Sb_5 : A Z_2 Topological Kagome Metal with a Superconducting Ground State, *Phys. Rev. Lett.* **125**, 247002 (2020).
- [34] H. Tan, Y. Liu, Z. Wang, and B. Yan, Charge Density Waves and Electronic Properties of Superconducting Kagome Metals, *Phys. Rev. Lett.* **127**, 046401 (2021).
- [35] Y. G. Zhong, S. Z. Li, H. X. Liu, Y. Y. Dong, K. Aidó, Y. Arai, H. X. Li, W. L. Zhang, Y. G. Shi, Z. Q. Wang *et al.*, Testing electron-phonon coupling for the superconductivity in kagome metal Cs_3V
 Sb_5 , *Nat. Commun.* **14**, 1945 (2023).
- [36] K. Fukushima, K. Obata, S. Yamane, Y. Hu, Y. Li, Y. Yao, Z. Wang, Y. Maeno, and S. Yonezawa, Violation of emergent rotational symmetry in the hexagonal Kagome superconductor CsV_3Sb_5 , *Nat. Commun.* **15**, 2888 (2024).
- [37] B. R. Ortiz, S. M. L. Teicher, L. Kautzsch, P. M. Sarte, N. Ratcliff, J. Harter, J. P. C. Ruff, R. Seshadri, and S. D. Wilson, Fermi Surface Mapping and the Nature of Charge-Density-Wave Order in the Kagome Superconductor
 CsV_3Sb_5 , *Physical Review X* **11**, 041030 (2021).
- [38] Y. Hu, X. Wu, B. R. Ortiz, S. Ju, X. Han, J. Ma, N. C. Plumb, M. Radovic, R. Thomale, and S. D. Wilson, Rich nature of Van Hove singularities in Kagome superconductor CsV_3Sb_5 , *Nat. Commun.* **13**, 2220 (2022).
- [39] M. Kang, S. Fang, J.-K. Kim, B. R. Ortiz, S. H. Ryu, J. Kim, J. Yoo, G. Sangiovanni, D. Di Sante, and B.-G. Park, Twofold van Hove singularity and origin of charge order in topological kagome superconductor CsV_3Sb_5 , *Nature Physics* **18**, 301 (2022).
- [40] R. Tazai, Y. Yamakawa, S. Onari, and H. Kontani, Mechanism of exotic density-wave and beyond-Migdal unconventional superconductivity in kagome metal $AV_3\text{Sb}_5$ ($A = \text{K}, \text{Rb}, \text{Cs}$), *Science Advances* **8**, eabl4108 (2022).